

EVALUATION OF THE WOUND HEALING PROCESS BY
IMMUNOHISTOCHEMISTRY AND PICROSIRIUS RED STAINING

A Thesis
Submitted to
the Temple University Graduate Board

In Partial Fulfillment
of the Requirements for the Degree
MASTER OF SCIENCE IN BIOENGINEERING

by
Junjie Lu
May 2017

Examining Committee Members:

Dr. Peter I. Lelkes, Advisory Chair, Department of Bioengineering

Dr. Yah-el Har-el, Department of Bioengineering

Dr. Cezary Marcinkiewicz, Department of Bioengineering

ABSTRACT

Non-healing wounds, also known as chronic wounds, are defined as wounds that do not show improvement in healing within four weeks. Chronic wounds affect millions of people around the world and health care expenses in the United States can cost more than one billion dollars. Chronic wound healing is a complicated process with different pathologies depending on the patients' condition. Four highly integrated and overlapping phases compose the wound healing process: hemostasis, inflammation, proliferation, and tissue remodeling. Occurrence of chronic wounds is usually due to unsuccessful progression through the normal stages of healing, and frequently enters a state of pathologic inflammation. Several cell types are involved in the wound healing process. Platelets initiate the coagulation cascade to stop the bleeding. Keratinocytes are able to restore the epidermis after injury. Vascular endothelial cells form the new blood vessels. Neutrophils and macrophages are responsible for phagocytosis and the release of growth factors and cytokines. Fibroblasts secrete collagen to fill the wound gap. Skin or tissue grafting is one of the many ways to treat non-healing wounds. Currently available skin substitutes have been proven successful in clinical trials, but they have room for improvement. Long-term culturing for cellularized scaffolds, risk of transferring disease from allogeneic or xenogeneic sources, and mismatching mechanical properties limit current skin substitutes in clinical applications. Given the disadvantages of those skin substitutes, plant protein can be a potent and attractive replacement material. Plant proteins can be extracted from renewable resources in abundance. Compared to skin substitutes from porcine or bovine sources, plant protein scaffolds do not have issues with immune rejection and can be formed into gels, films, or fibers with good bio-compatibility. Amongst the many plant proteins, soy protein is one of the ideal materials to make skin substitute scaffolds. Soy protein has been confirmed to be bio-active *in vivo* and *in vitro*. In this study, soy protein-based tissue scaffolds (SPS) were applied in full thickness excisional wounds in a porcine model. Immunohistochemistry (IHC) analysis was performed for macrophage invasion, newly formed vessel formation, and

picosirius red staining of collagen deposition. Results from IHC analysis show that SPS can accelerate the wound healing process.

Acknowledgements

I owe a great many thanks to a great many people who have helped me during this project.

First, I would like to express my gratitude to my thesis supervisors and committee members, Dr. Peter I. Lelkes, Dr. Yah-el Har-el and Dr. Cezary Marcinkiewicz for being great mentors. I learned a lot from you. Thanks for your guidance and your critical suggestions on my project.

Special acknowledgment should be given to Jonathan Gerstenhaber who helped me so much in my project. No matter what kind of problem I asked him, he can always give me some suggestions and always willing to help. Without his help, it would be so difficult for myself to finish my project. Brittney Wass is a very good friend and she was very patient when I learned different lab skills from her. I really appreciated learning from her and working with her in the lab. She also did a very good job on straightening out the linguistic issues for my thesis, which was a great help to me. I was very happy to work with Azadeh Timnak. She was willing to share her experience when I had some questions to ask her. Wuyan Li and Kang Dong are my good friends and colleagues and it was a great time to work with you in the lab.

My appreciation also goes to all the members of i-CTERM laboratory for their valuable help and suggestions during lab meetings. Thanks to Ms. Helen Freitas who is a great manager in our lab, managing everything when we need in the lab and training me how to culture cells. Last, I would like to say thank you to my family and friends who support me at this entire duration.

TABLE OF CONTENTS

ABSTRACT	ii
ACKNOWLEDGEMENTS.....	iv
LIST OF TABLES	vi
LIST OF FIGURES	vii
CHAPTER	
1. INTRODUCTION	1
2. AIM OF RESEARCH.....	8
2.1. Specific Aim	8
2.2. Hypothesis	8
2.3. Rationale	8
3. MATERIAL AND METHODS.....	10
3.1. Immunohistochemistry (IHC) – macrophages.....	10
3.2. Immunohistochemistry (IHC) – newly formed blood vessels.....	11
3.3. Picrosirius red staining	11
3.4. Image analysis	12
3.5. Statistical analysis.....	13
4. RESULTS	14
5. DISCUSSION	24
6. CONCLUSION AND FUTURE WORK	27
REFERENCES	28

LIST OF TABLES

Table	Page
1. Collagen deposition of soy and control group on a #182 porcine model.....	23
2. Collagen deposition of soy and control group on a #179 porcine model.....	23

LIST OF FIGURES

Figure	Page
1. Four phases of wound healing and the general time line.....	6
2. Diagram of M1 and M2 macrophages	7
3. Diagram of picosirius red image analysis	13
4. IHC staining of macrophages (L1).....	15
5. Macrophage count of soy treated wounds and control wounds on <i>in vivo</i> porcine model	15
6. IHC staining of newborn blood vessels (CD31)	16
7. Vessel count of soy treated wounds and control wounds on <i>in vivo</i> porcine model	17
8. Vessel area of soy treated wounds and control wounds on <i>in vivo</i> porcine model.	17
9. Vessel diameter of soy treated wounds and control wounds on <i>in vivo</i> porcine model	18
10. Wound width of soy treated wounds and control wounds on <i>in vivo</i> porcine model (#182).....	19
11. Wound width of soy treated wounds and control wounds on <i>in vivo</i> porcine model (#179).....	20
12. Collagen deposition of control wounds on a #182 porcine model.....	21
13. Collagen deposition of soy treated wounds on a #182 porcine model.....	21
14. Collagen deposition of control wounds on a #179 porcine model.....	22
15. Collagen deposition of soy treated wounds on a #179 porcine model.....	22
16. Correlation of vessel count and macrophage count.....	26

CHAPTER 1

INTRODUCTION

Skin substitutes are often used in the wound healing process. Cell-based dermal substitutes, epidermal substitutes or full thickness substitutes have been successfully used in clinical applications but their time-consuming cell culture and possible immune rejection restrict their application¹. Another skin substitute available is an acellular collagen scaffold. These collagen scaffolds are used in conjunction with fibroblasts or keratinocytes². However, these scaffolds contain animal-derived de-cellularized extracellular matrix and have the possibility of transferring intrinsic diseases¹. Moreover, some patients may reject using scaffolds that are derived from bovine and porcine material for religious or ethical reasons³.

Given the limitations of collagen scaffolds for use in the wound healing process, plant proteins can be an attractive potential replacement. Plant protein can be extracted from renewable sources in abundance. Furthermore, they also have the advantages of being non-toxic, biodegradable and able to form into different structures such as gels, films or fibers⁴.

Soy protein is one of the best examples of plant proteins that have shown their potential in pre-clinical studies. For example, cells remain viable when seeded on soy structures⁵ or grown in cell culture media with dissolved soy protein⁶. Human dermal fibroblasts can attach, grow and proliferate on fibrous mats electrospun from soy⁷. Soy granules made from defatted soy have the ability to stimulate collagen production and bone noduli mineralization *in vitro*⁸. All essential and non-essential amino acids present in soy protein affect its solubility and mechanical properties⁹. Hydrogen bonds, disulfide bonds and hydrophobic interactions in the molecular structure of soy protein are central to fabrication of gels¹⁰, films¹¹ or fibers¹². Recently an electrospun soy protein-based tissue scaffold (SPS) has been shown to enhance the wound healing process when SPS is applied in the full thickness excisional wound in the porcine model¹³. Therefore, soy protein scaffold is an ideal material to study the biological response *in vivo* and *in vitro*.

In the wound healing process, there are four highly programmed phases: hemostasis, inflammation, proliferation, and tissue remodeling¹⁴. The time for each phase is mainly depending on wound size and healing condition (figure 1). Ideal tissue repair needs these phases to occur not only at a precise time in relation to the initiation of a wound, but in specific sequence and intensity¹⁵. Delayed wound healing and non-healing chronic wounds are the results of aberrations occurring in these four phases. In the hemostasis phase, vessels constrict and a fibrin clot starts to form immediately after wounding. Vascular constriction and fibrin clots help stop bleeding and release pro-inflammatory cytokines such as transforming growth factor (TGF)- β , platelet-derived growth factor (PDGF) and fibroblast growth factor (FGF) to attract inflammatory cells to the wound, programming to the inflammatory phase¹⁴.

Neutrophils, macrophages, and lymphocytes are the hallmark of the inflammatory phase. When these cells are attracted to the wound, they serve their function by clearing invading microbes and cellular debris^{16,17}. Macrophages in this phase not only play a role in promoting inflammatory responses by releasing cytokines to recruit and activate additional leukocytes, but they also can differentiate to a reparative phenotype to prepare for the proliferation phase^{18,19}. Macrophages are the bridge that connects the inflammation and proliferation phases. In the proliferation phase, endothelial cells and fibroblasts are the major active cells in the wound site and they are responsible for the formation of provisional matrix, which includes capillary growth, collagen formation, and the formation of granulation tissue.

Glycosaminoglycans and proteoglycans are two major components in extracellular matrix (ECM) and are produced by fibroblasts in the proliferation phase¹⁴. Lastly, in the remodeling phase, collagen that is deposited in the provisional matrix is remodeled and newly formed vessels go through maturation and regression. The remodeling phase is programmed to draw back the capillary intensity to normal and make the architecture of the ECM in the wound close to that of normal tissue. The remodeling phase usually takes months to years and the physical contraction throughout the wound healing process is mediated by myofibroblasts^{14,17}.

Angiogenesis is an important part in wound healing. In the proliferation phase, granulation tissue will form, which consists of fibroblasts, macrophages, endothelial cells that will form a dense network of capillary loops²⁰. These loops originate from the wound margin and spread into the wound bed by the vigorous angiogenic response²¹. As the wound heals over several days or weeks, the density of blood vessels in the wound bed increases and can reach greater than three times higher than that of normal and uninjured tissues²². The temporary fibrous matrix, which is secreted by fibroblasts and is rich in collagen type III, helps endothelial cells penetrate the matrix during sprouting²³. As a result, the neo-vascular network is quickly formed. However, most of the newly formed vessels are functionally immature and their architecture is twisted²⁴ because there are not enough pericytes to cover them as the endothelial cell-endothelial cell contact is not tight in these neo-vessels²⁵. Therefore, these barely perfused and leaky new-vessels lead to the appearance of wet granulation tissue²⁶.

In the remodeling phase, the provisional, angio-permissive collagen type III-rich ECM is breaking down, as programmed, and is replaced with collagen type I- the primary component in pre-wounded, angio-restrictive ECM²⁰. Meanwhile, further vessel sprouting is prevented and regression of the vessels is initiated²⁷. To draw the density of blood vessels in the wound back to baseline levels, only a minority of newly formed vessels can undergo maturation²⁸ and are integrated into the existing perfused network while most of the neo-vessels are predisposed to pruning²⁹.

Fibroblasts are attracted to the wound site by the cytokines released from neutrophils and macrophages and form the provisional ECM. Increased numbers of fibroblasts lead to increased collagen synthesis and contraction³⁰. Myofibroblasts are a specialized form of fibroblast which are also involved in collagen synthesis³¹. The major function of fibroblasts is producing and remodeling the ECM in order to maintain the physical integrity of connective tissue³², while myofibroblasts are working to produce a dense and fibrotic collagen matrix³³. α -smooth muscle actin (SMA), collagens type I, III, IV and V are the products of myofibroblasts³³. In the wound healing process, collagen

type I and III are two predominant collagens and myofibroblasts synthesize more collagen type III than collagen type I in the granulation tissue³⁴. As the wound is switching to the remodeling phase, collagen type III deposition is decreasing and collagen type I is increasing, resulting in a large amount of collagen type I scar tissue³⁵. Excessive deposition of collagen type III in the remodeling phase may lead to hypertrophic and keloid scars³⁰.

Macrophages are one of the most important cell types in the wound healing process and are active in all four major phases of wound healing¹⁴. M1 and M2, which are the two types of macrophages, are responsible for specific concepts in the wound healing process (figure 2). Characterizations of M1 macrophages are their abilities to produce high levels of pro-inflammatory cytokines and reactive nitrogen and oxygen intermediates. Parasite control, tissue remodeling, immune regulation and tumor promotion are characterizations of M2 macrophage phenotype³⁶. Macrophages can be found in tissue or peripheral blood. For many years, macrophages were considered to be derived solely from circulating monocytes. These monocytes are derived from the common precursor cells in the bone marrow. However, recent studies show that some tissue resident macrophages are probably generated during the embryological development³⁷. These tissue resident macrophages are sustained by rapid proliferation during injuries. Monocytes will also differentiate into macrophages after they leave the bone marrow microenvironment and enter the circulating peripheral blood system. When tissues are inflamed, macrophages will be recruited to that area, activate and exhibit a spectrum of polarization states. Each polarization state has its own functional diversity. There are two typical states in this spectrum. One is the pro-inflammatory M1 state and the other is the anti-inflammatory M2 state³⁸ (Figure 2).

M1 macrophage (also cknown as inflammatory macrophages) can be activated by many factors, such as the bacterial lipopolysaccharide (LPS), interferon- γ (IFN- γ), microbial products, and molecular fragments of ECM³⁹. M2 refers to “regenerative” or “reparative” macrophages that are activated by the interleukins 4 and 13 (IL-4, IL-13). Their tasks include immune-regulatory and tissue remodeling. Recent studies show that diversity and plasticity of macrophages in wound

healing are dependent on the types of materials used for implantation⁴⁰. In addition, the ratio between M1 and M2 at different points of time and their position in the wound can be an indicator of wound healing.

M1 macrophages can present a large number of antigens as well as promote lymphocytes to differentiate into type 1 helper T cells (Th1) form, which can produce pro-inflammatory cytokines that react with intracellular pathogens⁴¹. M1 macrophages produce toxic reactive oxygen intermediates and escalate the pro-inflammatory response, which also may cause some damage to the neighboring cells in the microenvironment⁴². When implanting a regenerative biomaterial to replace lost tissue, a prolonged M1 macrophage presence is undesirable because it will lead to a severe foreign body reaction, granuloma and fibrous encapsulation, which usually ends in chronic inflammation and failure of the biomaterial integration⁴³.

M2 phenotype macrophages become active as a result of a series of signals that come mostly from basophils, mast cells and other granulocytes⁴⁴. In the process of remodeling, different subsets of M2 macrophages play different roles in the process. Functions of M2a and M2b are to perform immune regulation by initiating the anti-inflammatory response. M2a can indirectly produce TGF- β , which is a powerful activator for fibroblasts to produce collagen⁴⁵, and directly synthesize ECM components such as collagen type VI and fibronectin^{46,47}. M2c is capable of tissue remodeling and suppression of inflammatory immune reactions by secreting cytokines, transforming growth factors, and interleukin. The tissue remodeling response and the cytokines coming from M2 macrophages can prohibit the formation of fibrous tissue, thus supporting the vascularization of regenerative biomaterials and improve its integration.

Macrophages can switch polarization states when changes occur in their microenvironment. This temporary ability is related to their paracrine signaling mechanism. M1 macrophages can produce IL-12, but IL-12 can be dampened by the presence of IL-4, a M2 polarizing cytokine that is secreted by M2 macrophages. Therefore, the presence of M2 macrophages will have a negative effect on M1 macrophages⁴⁸, i.e. reduce the number of M1 macrophages and thus enhance tissue

remodeling/repair⁴⁸. Although some researches show that a high M2:M1 ratio in the area where biomaterials are implanted leads to a better remodeling outcome, prolonged existence of M2 macrophages can be detrimental, resulting in foreign body giant cells. Therefore, a better understanding of the M2:M1 ratio can help us design an improved biomaterial to advance tissue remodeling, integration and regeneration.

As mentioned above, soy protein can be formed into gels¹⁰, films¹¹ or scaffolds¹². Soy protein derived wound matrices are biocompatible *in vivo*⁵. SPS have been proven to accelerate wound healing in a porcine model¹³. Soy proteins are associated with fatty acids, saponins, isoflavones and phospholipids⁴⁹. The concentration of isoflavones in soy proteins is the largest among the plant based proteins⁵⁰ and may be one of the reasons why SPS has the ability to accelerate wound healing. In a mouse model, monocytes and lymphocytes were affected by isoflavones, showing their anti-inflammatory properties.⁵¹

Macrophages serve different functions in specific phases of the wound healing process. The mechanism of how SPS and other soy structures affect wound healing is still unknown but isoflavones in soy protein may play a vital role in activating macrophages. In this study, macrophages, blood vessels, and collagen deposition will be parameters to analyze how the wound is healing.

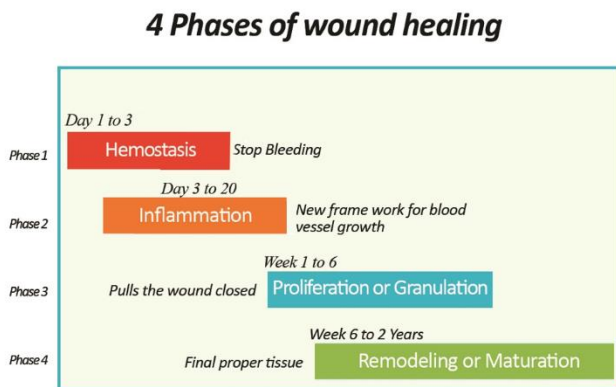


Figure 1. Four phases of wound healing and the general timeline (Image credit: www.woundeducators.com).

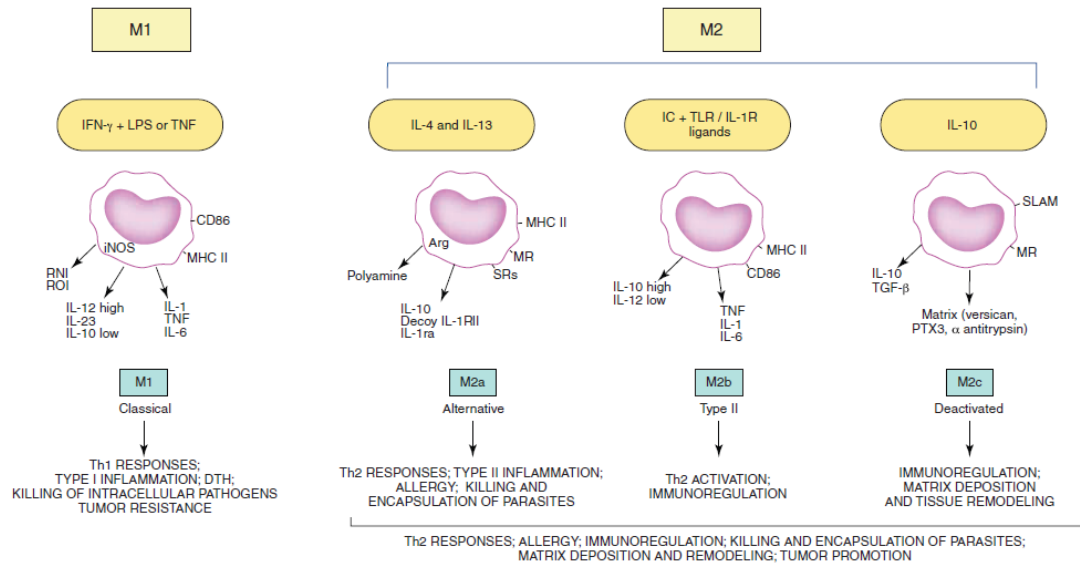


Figure 2. Diagram of M1 and M2 macrophages (Martinez, F. O., & Gordon, S. (2014). The M1 and M2 paradigm of macrophage activation: time for reassessment. *F1000Prime Rep*, 6(13.10), 12703.)

CHAPTER 2

AIM OF RESEARCH

- 2.1 **Specific aim:** To investigate the wound healing process of a porcine model at weeks 1, 2 and 4 post-surgery, by counting macrophages and newly formed blood vessels and analyzing collagen deposition in the wound.
- 2.2 **Hypothesis:** The basis of the research is to use IHC staining to detect macrophages and newly formed blood vessels and picosirius red staining to evaluate collagen deposition in wound. With these factors, we will be able to quantitatively assess the wound healing process I hypothesize that a wound treated with SPS will heal faster than a control wound just covered by a state-of-the art wound dressing (Tegaderm®) and not treated with SPS.
- 2.3 **Rationale:** Although there are four different phases that compose the wound healing process and overlap with one another, each phase has its distinct symptoms. Macrophages are the key cell type involved in the wound healing process⁵². Their functions include debriding the damaged tissue and phagocytosing bacteria and foreign material⁵³ during the inflammation phase. Not only can macrophages clear exogenous matter but they also secrete growth factors and cytokines to attract and activate vascular endothelial cells for angiogenesis⁵⁴ or fibroblasts for collagen deposition in the proliferation phase⁵⁵. Angiogenesis is a physical process in which blood vessels form from the pre-existing ones⁵⁶. As endothelial cells are activated by growth factors from macrophages, they can loosen themselves from their embedded endothelium, divide, migrate towards the wound and lay down new vessels⁵⁷. Density of blood vessels in the wound will reach a peak in the proliferation phase and gradually regress to a normal level in the remodeling phase²². As fibroblasts start to produce collagen in the wound and build a provisional matrix, cells involved in the wound healing process attach to, grow and differentiate

on it⁵⁸. Fibronectin and collagen type III are two proteins that are produced in the beginning of the wound healing process but collagen type I becomes dominant as the wound enters the remodeling phase⁵⁹. Production of collagen is a dynamic process. For example, new collagen is produced by fibroblasts while collagenases in the wound degrade them. The speed of synthesizing new collagen is faster than the degradation in the beginning of the wound healing process and becomes equal in the late phase so there will not be net collagen gain⁵⁴.

CHAPTER 3

MATERIAL AND METHODS

Analysis of the samples by immunohistochemistry was carried out using paraffin sections of pig tissue that were collected in an animal study performed by other members of the lab. Samples were collected from 1, 2, and 4 week old wounds post-surgery. The primary antibody against M1 macrophages was goat anti-CCR7 IgG (a receptor for chemokine ligand 19/21, Novus) at a dilution of 1:200. The primary antibody against M2 macrophages was rabbit anti-CD206 IgG (mannose receptor, Bioss) at a dilution of 1:200. The primary antibody against pan-macrophages was mouse anti-L1 IgG at the dilution of 1:100. The secondary antibodies were anti-goat IgG at a dilution of 1:200, anti-rabbit IgG and anti-mouse IgG at a dilution of 1:200 respectively. The primary antibody against newly formed blood vessels was rabbit anti-CD31 IgG (Abcam) at a dilution of 1:50. The secondary antibody was anti-rabbit IgG at a dilution of 1:200. Samples were stained with the Vectastainv ABC immunoperoxidase kit using 3,3'-diaminobenzidine (DAB) as the substrate (Vector Laboratories, Inc).

3.1 Immunohistochemistry (IHC) - Macrophages

Paraffin samples (5 μm) were treated for antigen retrieval with 0.25 % trypsin (Cellgro) at 37 °C for 10 minutes after rehydration and washed twice with TBST (Tris buffered saline with 0.05 % Triton X-100). Then the samples were incubated with a blocking solution (10 % FBS) for 1 hour at room temperature. Samples were incubated with the primary antibody overnight at 4 °C. For a negative control, samples were not treated with primary antibody but antibody dilution buffer instead. The samples had the primary antibody drained off and were incubated with 0.3 % hydrogen peroxide for 15 minutes. Samples were washed twice for 5 minutes each with TBST and then incubated with the secondary antibody for 1 hour at room temperature. Following washing twice for 5 minutes each time with TBST, samples were incubated with the ABC solution for 30 minutes

and then with DAB solution until color was visible as the manufacturer instructed. Counterstaining samples in hematoxylin was done to increase contrast. Slides were dehydrated in 80% ethanol, 90% ethanol, absolute ethanol, xylene for 1 minute in each solution. Dehydrated slides were mounted in Richard-Allan Cytoseal-60 mounting medium and cover-slipped before imaging. All images were taken using Olympus Microscope with a Digital Camera Model DP26 at 10X magnification.

3.2 Immunohistochemistry (IHC) - Newly-formed Blood Vessels

The method to stain newly formed blood vessels was similar to staining macrophages, with minor modifications: In brief, in the antigen retrieval step, samples were put in the antigen retrieval buffer overnight at 65 °C after rehydration. This antigen retrieval buffer is composed of 0.294 g trisodium citrate dihydrate ($\text{Na}_3\text{C}_6\text{H}_5\text{O}_7$) dissolved in 100 mL distilled and di-ionized water (DD water). Tween 20 (50 μL) was added after the pH of the solution was adjusted to 6.0. The concentration of the blocking solution was 1 % FBS. Other steps and solutions were the same as in IHC staining of macrophages. The primary antibody used was rabbit anti-CD31 at a dilution of 1:50. The secondary antibody was anti-rabbit IgG at a dilution of 1:200.

3.3 Picrosirius Red Staining

Collagen was analyzed in samples from the same tissue sections respective to immunohistochemistry analysis. A picrosirius red stain kit (Polyscience, Inc) and Weigert's iron hematoxylin working solution was used. The Weigert's iron hematoxylin working solution was a mix of two stock solutions A and B. Solution A was 2 g hematoxylin dissolved in 200 mL 95 % ethanol and solution B was 8 mL 29% aqueous ferric chloride and 2 mL concentrated hydrochloric acid mixed with 190 mL DD water. After A and B were prepared, they were mixed in a ratio of 1:1 to make the Weigert's iron hematoxylin working solution.

Paraffin samples were dipped into the following solutions (10 minutes for each solution): Xylene, Xylene, mix of 50% Xylene and 50% Ethanol, absolute Ethanol, absolute Ethanol, 90% Ethanol, 80% Ethanol, and 70% Ethanol. After rehydration, they were put in tap water for 5 minutes and then stained with Weigert's iron hematoxylin working solution for 10 minutes. Samples were rinsed again in tap water for 5 minutes and tap water was changed every minute while rinsing. Afterwards, samples were rinsed in DD water 2 times, for 5 seconds each. Then samples were stained using the picosirius red staining kit, following the instruction from the manufacturer. There were three different solutions in the kit and samples were rinsed in DD water for 5 seconds while changing samples from one solution to another. After staining using the picosirius red staining kit, samples were dehydrated in 90 % ethanol, absolute ethanol and xylene for 20 seconds each. Sample were mounted in Richard-Allan Cytoseal-60 mounting medium and cover-slipped before imaging.

3.4 Image analysis

To analyze IHC images of L1 staining that is for macrophages, a hot spot was defined first on the image where density of the brown stained macrophages was the highest. Then 5 equally sized areas ($275.48 \times 275.48 \text{ um}^2$) were chosen in the hot spot. These areas were inversed to black and white by the image process software ImageJ and the black dots represented the macrophages. Total count of black dots represented the total count of macrophages in the area.

To analyze IHC images of CD31 staining that is for newly formed vessels, 5 equally sized areas ($694.44 \times 694.44 \text{ um}^2$) were chosen in the wound. To count vessels and their areas, circles were drew around the brown stained vessels by hand in imageJ. To count vessel diameters, lines were drawn across the brown stained vessels by hand in ImageJ.

To analyze picosirius red images, a line was drawn through the whole tissue to collect the grey value at each pixel along a line that was 1mm from the skin surface (Figure 1). Each pixel generated

a value, resulting in over 10,000 data points per image, depending on the specific size of the tissue. Data points were extracted from the grey value data at every 100 pixels (~100 values) and an inverse of each grey value was used so that the largest data values represented the reddest pixels and the smallest data values represented the wounded area of the tissue. These values were normalized from 0 to 1 and represented the weakest to strongest red signals. All images were processed in Image J.

3.5 Statistical analysis

Data are expressed as mean \pm standard deviation. A one tail t-test was used to determine significance.

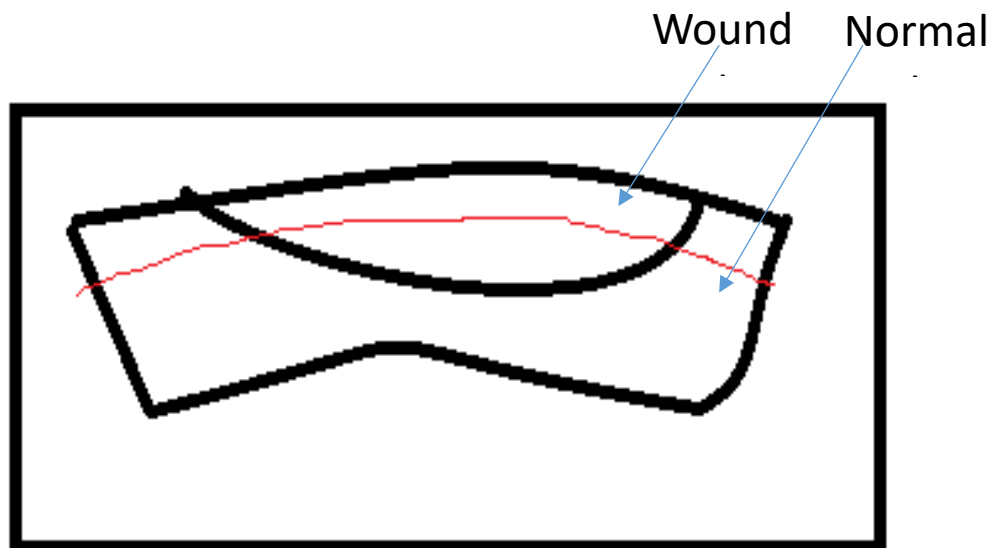


Figure 3. Diagram of picrosirius red image analysis. The image shows a representative wounded tissue. The red line shows how a line was drawn through the whole tissue 1mm from the surface. Data from the images represented different collagen deposition in the whole tissue.

CHAPTER 4

RESULTS

To count the number of macrophages in each wound, the stitched images of each wound were analyzed with ImageJ software. Hot spots were defined as areas of the wound with a dense distribution of macrophages. For each image, 5 areas were chosen in the hot spot and macrophages were counted in those areas using a specific protocol described in image analysis. Figure 4 shows representative hot spots of each wound for L1, the pan-macrophage marker in A, B, C, D and F. There were no visible hotspots in Figure 4E and therefore 5 areas were randomly chosen in the wound area to count macrophages.

The average amounts of macrophages counted were 134, 115 and 4 in weeks 1, 2 and 4 of the soy treated group, respectively (Figure 5). The average amounts of macrophages were 150, 59 and 44 in week 1, 2 and 4 of the control group respectively. In week 2 vs week 4, the amount of macrophages dropped significantly in the soy treated group. Compared to the control group, the soy group in week 4 has significantly less macrophages.

The blood vessel count of the soy and control groups both decreased with time (Figure 7). In figure 6, the brown stained irregular circles showed the position of newly formed vessels in the wound. Compared 6A and 6E, 6B and 6F, density of newly formed vessels was lower in week 4 in both wound types. The number of blood vessels in the soy treated wounds in week 1, 2 and 4 were 74, 71 and 38, respectively. In the control wounds in week 1, 2 and 4, the numbers of blood vessels were 74, 63 and 44 respectively. Comparing week 1 with week 2, neither group had a significant difference in vessel count. Comparing week 2 and week 4, both groups significantly decreased in vessel count. The number of vessels counted in normal skin of the same size was 24.

Vessel area of soy treated wounds decreased from week 1 to week 4 (Figure 8). Average vessel area of soy group was $1438 \mu\text{m}^2$, $768 \mu\text{m}^2$ and $463 \mu\text{m}^2$ for week 1, 2 and 4 respectively. There is significant difference between week 1 and week 2 as well as week 2 and week 4. Average vessel

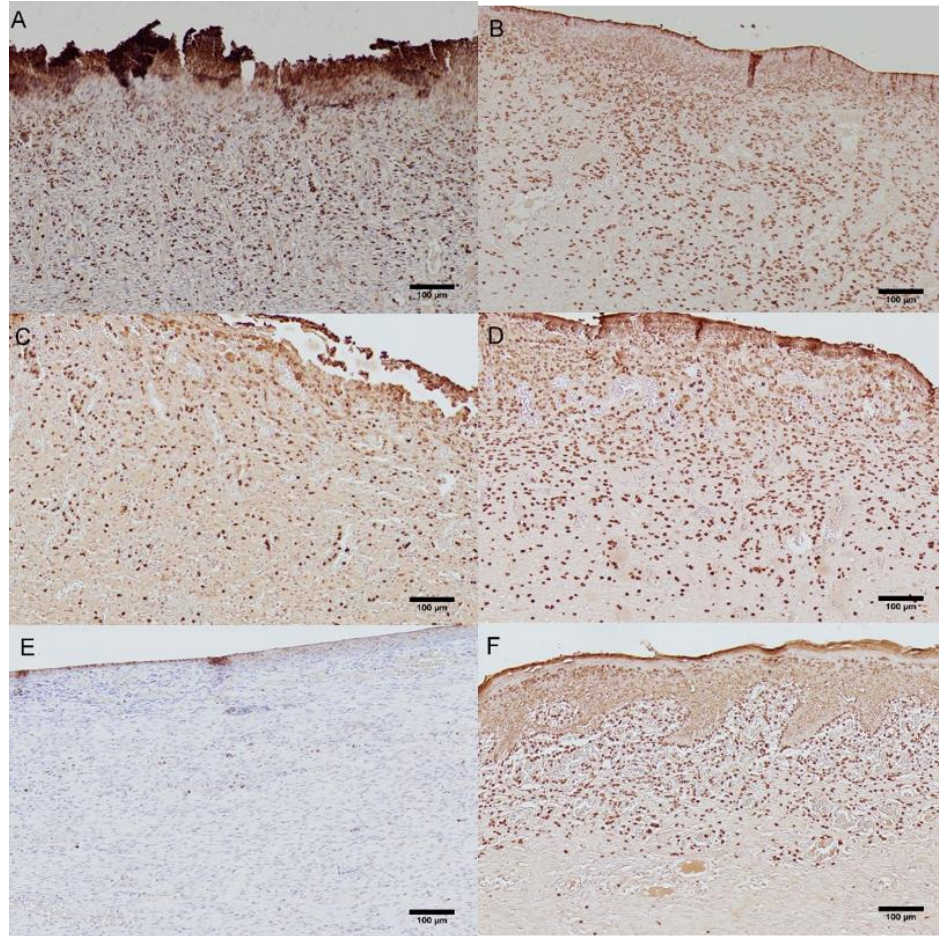


Figure 4. IHC staining of macrophages (L1). Representative images of A. Soy treated wound in week 1 B. Control wound in week 1 C. Soy treated wound in week 2 D. Control wound in week 2 E. Soy treated wound in week 4 F. Control wound in week 4. Scale bar is 100 μm . Brown cells show stained macrophages and the blue dots are the stained nuclei. Images B, C, D, F were observed to have light blue stained nucleus or no staining due to bad counterstaining. Images were taken at 10X.

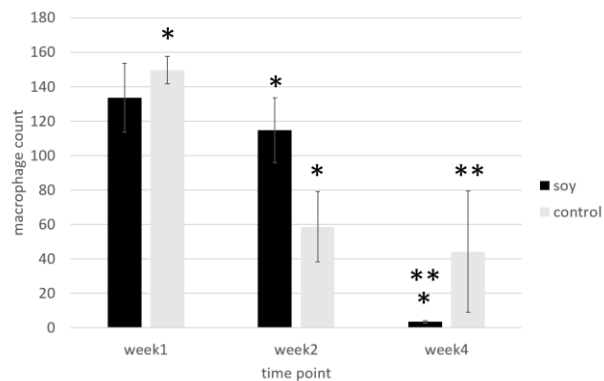


Figure 5. Macrophage count of soy treated wounds and control wounds in a porcine model (pig #182). Week 1 and week 2 analyzed 6 images and week 4 analyzed 4 images. In each wound image, 5 areas of the same size ($275.48 \times 275.48 \mu\text{m}^2$) were chosen to count macrophages. The data presents the average \pm SD of measurements of macrophages. * $p < 0.01$ The count of macrophages in soy week 2 compared to soy week 4 and the count of macrophages in control week 1 compared to control week 2. ** $p < 0.01$ The count of macrophages in soy week 4 compared to control week 4.

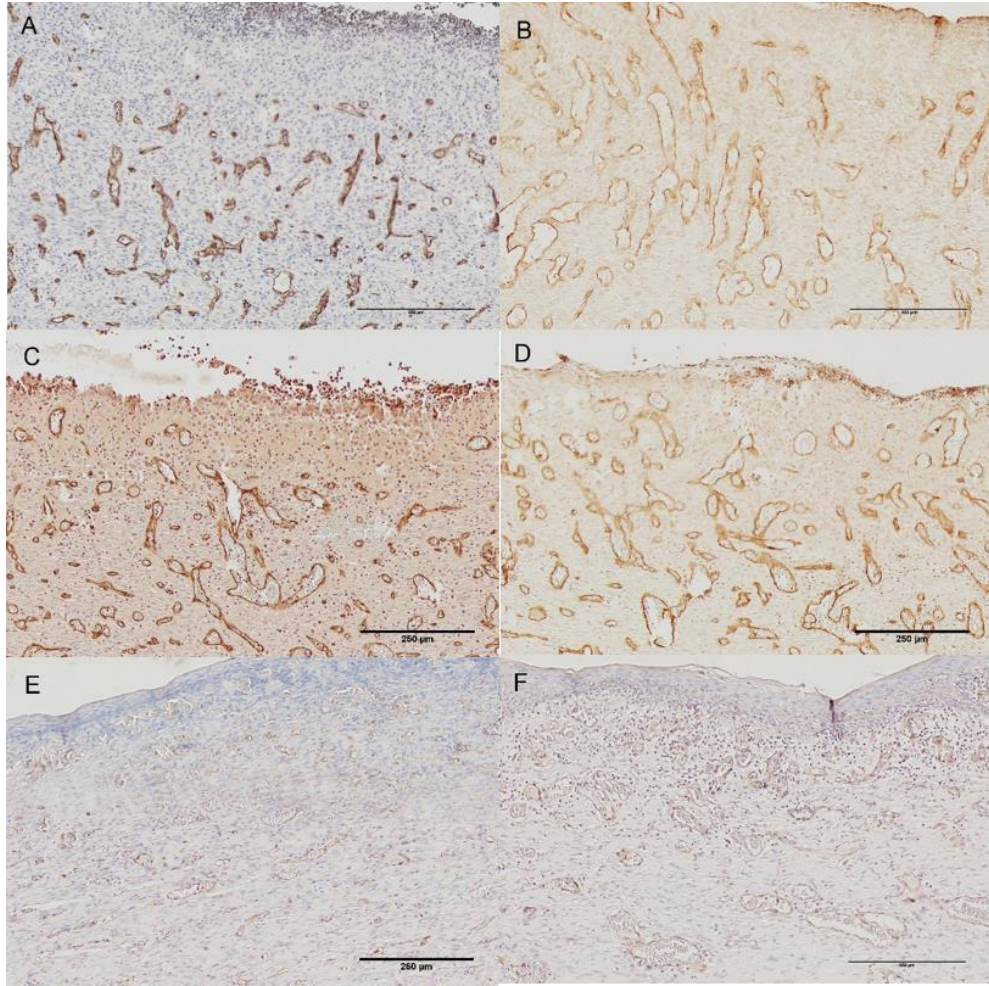


Figure 6. IHC staining of newborn blood vessels (CD31) A. Soy treated wounds in week 1 B. Control wounds in week 1 C. Soy treated wounds in week 2 D. Control wounds in week 2 E. Soy treated wounds in week 4 F. Control wounds in week 4. Scale bar is 250 μm . The irregular brown circles are stained blood vessels. The blue dots are stained nucleus. B, C and D did not have nuclear staining because of poor counterstaining. Images were taken at 10X. Area is $694.44 \times 694.44 \mu\text{m}^2$

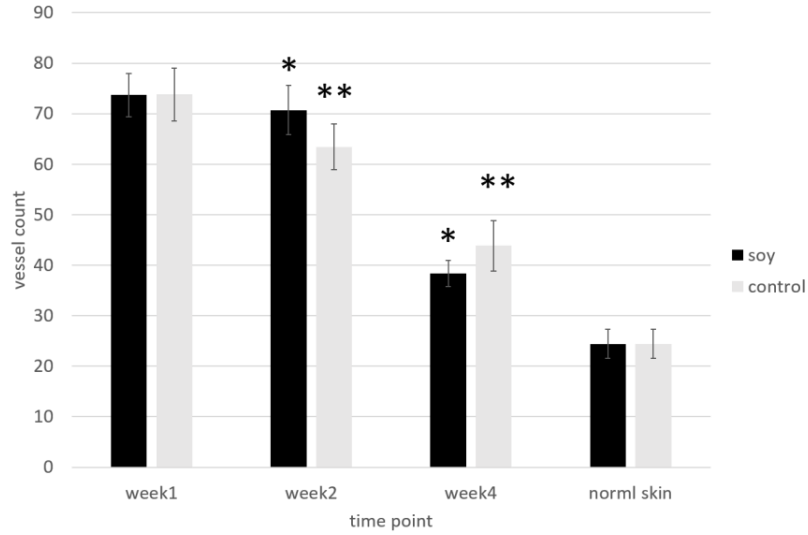


Figure 7. Vessel count of soy treated wounds and control wounds on a #182 porcine model. Week 1 and week 2 have 6 images and week 4 has 4 images. 5 areas were chosen to count vessels in the wound part of each image and these areas are the same. Area is $694.44 \times 694.44 \text{ um}^2$. The data presents the average \pm SD of measurements of vessels. * $p < 0.01$ The count of vessels in soy week 2 compared to soy week 4. ** $p < 0.01$ The count of vessels in control week 2 compared to control week 4.

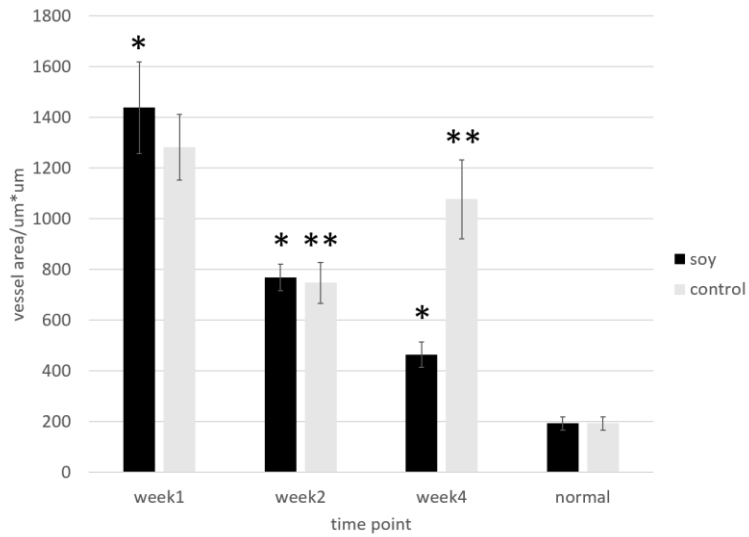


Figure 8. Vessel area of soy group and control group on a #182 porcine model. Week 1 and week 2 have 6 images and week 4 has 4 images. 5 areas were chosen to count vessels area in the wound area of each image and these areas are the same. Area is $694.44 \times 694.44 \text{ um}^2$. The data presents the average \pm SD of measurements of vessels area. * $p < 0.01$ The vessel area in soy week 1 compared to soy week 2 and week 2 compared to soy week 4. ** $p < 0.01$ The vessel area in control week 2 compared to control week 4.

area of control group was 1283 μm^2 , 747 μm^2 and 1077 μm^2 for week 1, 2 and 4 respectively. Week 2 and week 4 had significant difference. Vessel area in normal skin was 192 μm^2 .

Vessel diameters of the control group decreased between week 1 and week 2 but slightly increased between week 2 and week 4 (Figure 9). Average vessel diameter in the control group wounds were 25 μm , 19 μm and 22 μm for week 1, 2 and 4 respectively. Comparing control week 1 and week 2, there was a significant difference. Soy group from week 1 to week 4 decreased and a significant difference was found between week 2 and week 4. Average vessel diameter of soy group was 22 μm , 20 μm and 14 μm for week 1, 2 and 4 respectively. In normal skin, the average vessel diameter was 9 μm .

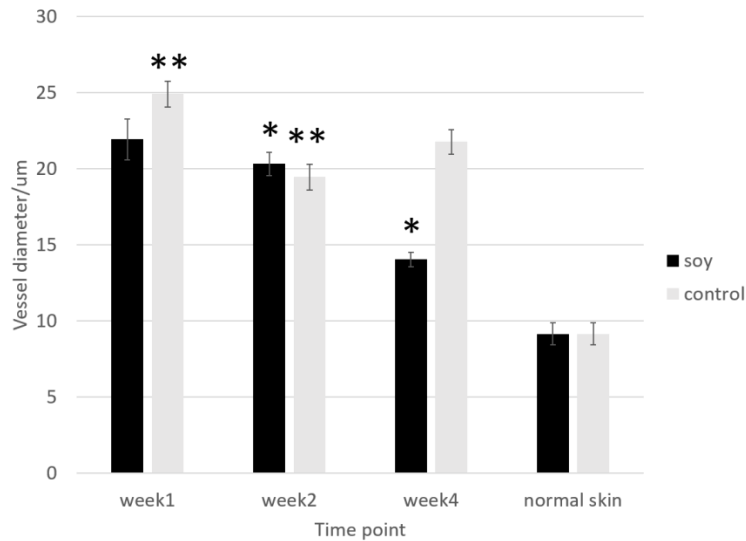


Figure 9. Vessel diameter of soy treated wounds and control wounds on a #182 porcine model. Week 1 and week 2 have 6 images and week 4 has 4 images. 5 areas were chosen to count vessel area in the wound area of each image and these areas are the same. Area is 690.61×690.61 μm^2 . The data presents the average \pm SD of measurements of vessels diameter. * $p < 0.01$ The vessel diameter in soy week 2 compared to soy week 4. ** $p < 0.01$ The vessel diameter in control week 1 compared to control week 2.

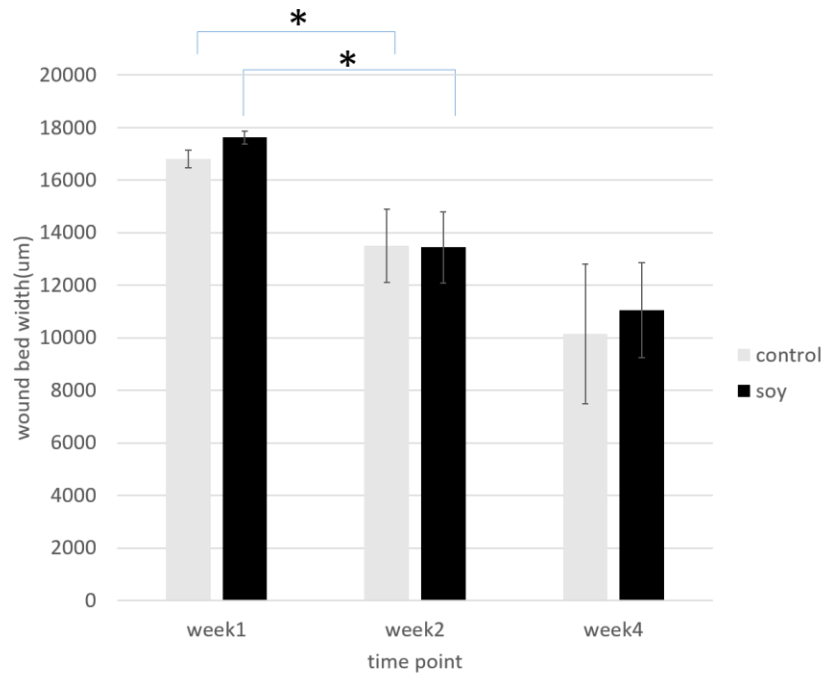


Figure 10. Wound width of soy treated wounds and control wounds on a #182 porcine model. The data presents the average \pm SD of wound width. Each type of wound has more than 4 images to measure. * $p < 0.01$ The wound width in soy week 1 compared to soy week 2 and the wound width in control week 1 compared to control week 2.

Wound width of control wounds on #182 pig model were 16799 um, 13503 um and 10134 um for week 1, 2 and 4 respectively. Wound width of soy treated wounds on #182 pig model were 17620 um, 13439 um and 11043 um for week 1, 2 and 4 respectively. Wound width of both wound types decreased week 1 to week4 and they drop significantly from week 1 to week 4.

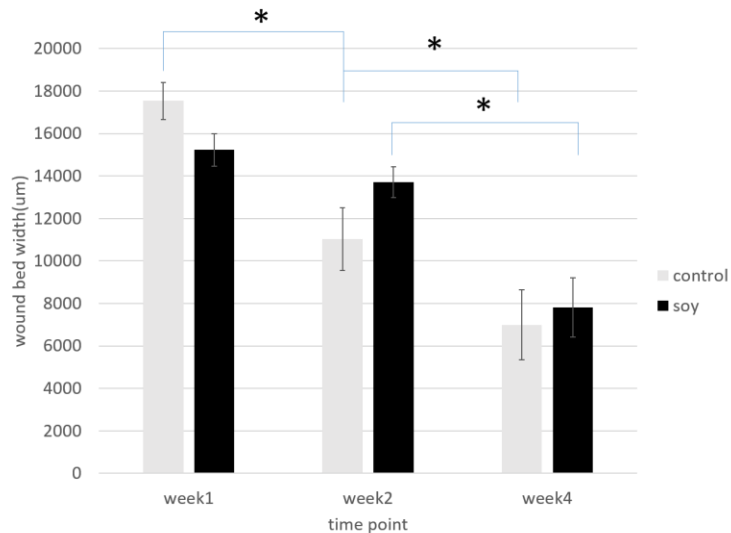


Figure 11. Wound width of soy treated wounds and control wounds on a #179 porcine model. The data presents the average \pm SD of wound width. Each type of wound has more than 4 images to measure. * $p < 0.01$ The wound width in soy week 2 compared to soy week 4, control week 1 compared to control week 2 and control week 2 compared to control week 4.

Wound width of control wounds on #179 pig model were 17536 um, 11037 um and 6990 um for week 1, 2 and 4 respectively. Wound width of soy treated wounds on #179 pig model were 15227 um, 13720 um and 7809 um for week 1, 2 and 4 respectively. Wound width of control wounds on #179 pig decreased from week 1 to week 4 and it dropped significantly from week 1 to week 2 and week 2 to week 4. Wound width of soy treated wounds also decreased from week 1 to week 4 but it only dropped significantly from week 2 to week 4.

After raw data were collected from images, they were normalized as 0 to 1, representing the blank to the reddest in the images. The data was then separated into groups from 0-0.1, 0.1-0.2, etc. Total amount of data in each group was summarized to plot shown in figure 12, 13, 14 and 15. Table 1 and 2 shows how collagen was deposited throughout the whole tissue.

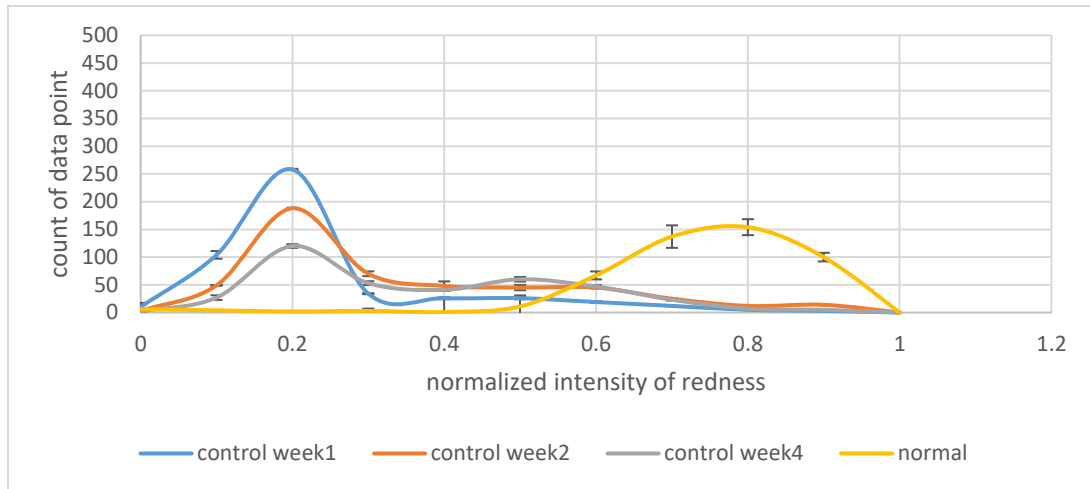


Figure 12. Collagen deposition of control wounds on a #182 porcine model. The X axis represents the normalized intensity of redness of picosirius red stained tissue. 0 is the blank and 1 is the reddest in the stained tissue. The Y axis represents the count of data that fall into 0-0.1, 0.1-0.2, 0.2-0.3, ... , 0.8-0.9 or 0.9-1. The data presents the average \pm SD of count of data point. Each type of wound measured three times.

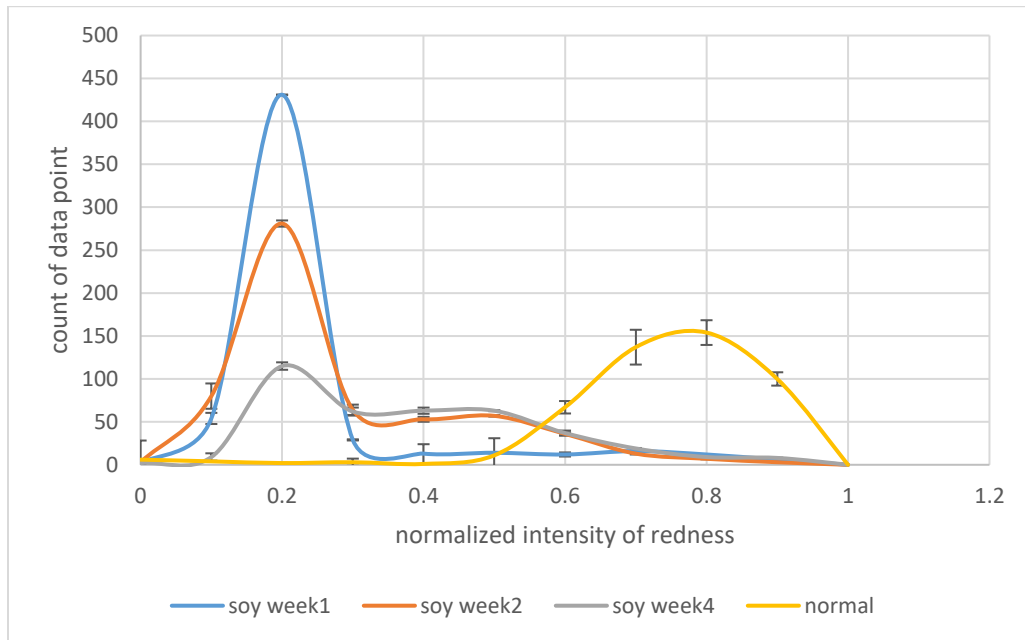


Figure 13. Collagen deposition of soy treated wounds on a #182 porcine model. The X axis represents the normalized intensity of redness of picosirius red stained tissue. 0 is the blank and 1 is the reddest in the stained tissue. The Y axis represents the count of data that fall into 0-0.1, 0.1-0.2, 0.2-0.3, ... , 0.8-0.9 or 0.9-1. The data presents the average \pm SD of count of data point. Each type of wound measured three times.

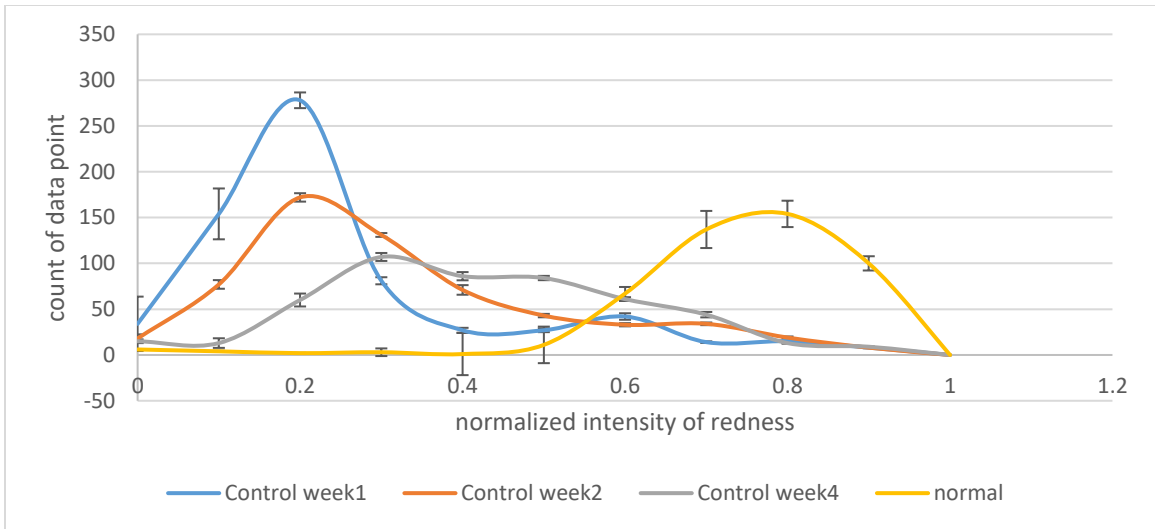


Figure 14. Collagen deposition of control wounds on a #179 porcine model. The X axis represents the normalized intensity of redness of picosirius red stained tissue. 0 is the blank and 1 is the reddest in the stained tissue. The Y axis represents the count of data that fall into 0-0.1, 0.1-0.2, 0.2-0.3, ... , 0.8-0.9 or 0.9-1. The data presents the average \pm SD of count of data point. Each type of wound measured three times.

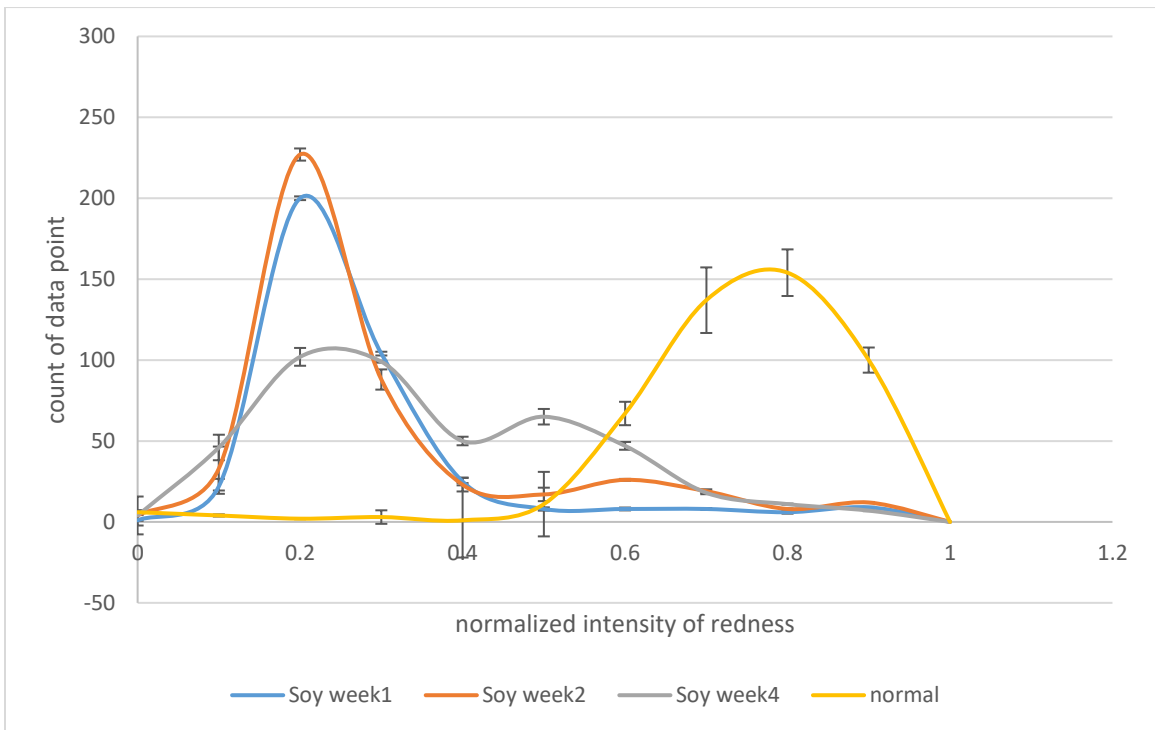


Figure 15. Collagen deposition of soy treated wounds on a #179 porcine model. The X axis represents the normalized intensity of redness of picosirius red stained tissue. 0 is the blank and 1 is the reddest in the stained tissue. The Y axis represents the count of data that fall into 0-0.1, 0.1-0.2, 0.2-0.3, ... , 0.8-0.9 or 0.9-1. The data presents the average \pm SD of count of data point. Each type of wound measured three times.

Table 1. The collagen deposition of soy treated wounds and control wounds on a #182 porcine model. Data represents the ratio of counted data that fall in the ranges 0-0.3, 0.3-0.6 or 0.6-1 to the total counted data. The data presents the average \pm SD. Each type of wound measured three times

range	control			soy			normal
	week1	week2	week4	week1	week2	week4	
0-0.3	81.7% \pm 0.5%	62.1% \pm 1.6%	52.5% \pm 1.3%	87.6% \pm 0.4%	71.7% \pm 1.5%	48.6% \pm 1.6%	3.1% \pm 0.1%
0.3-0.6	14.3% \pm 0.5%	27.7% \pm 1.6%	38.4% \pm 0.6%	6.6% \pm 0.1%	24.5% \pm 1.2%	42.1% \pm 1.9%	16.3% \pm 9.8%
0.6-1	4% \pm 0.3%	10.2% \pm 0.2%	9.1% \pm 0.7%	5.8% \pm 0.5%	3.9% \pm 0.3%	9.3% \pm 0.8%	80.6% \pm 9.9%

Table 2. The collagen deposition of soy and control groups on a #179 porcine model. Data represents the ratio of counted data that fall in the ranges 0-0.3, 0.3-0.6 or 0.6-1 to the total counted data. The data presents the average \pm SD. Each type of wound measured three times

range	control			soy			normal
	week1	week2	week4	week1	week2	week4	
0-0.3	80.4% \pm 0.3%	65.7% \pm 1.4%	39.6% \pm 0.8%	83.4% \pm 0.2%	76.9% \pm 0.3%	55.9% \pm 0.1%	3.1% \pm 0.1%
0.3-0.6	14.1% \pm 0.5%	24.3% \pm 1.1%	47.0% \pm 0.6%	10.5% \pm 0.2%	14.4% \pm 0.2%	36.1% \pm 0.4%	16.3% \pm 9.8%
0.6-1	5.4% \pm 0.5%	10.1% \pm 0.3%	13.4% \pm 0.3%	6.1% \pm 0.3%	8.7% \pm 0.2%	8.0% \pm 0.4%	80.6% \pm 9.9%

CHAPTER 5

DISCUSSION

In the hemostasis and the inflammation phase, macrophages serve to remove damaged tissues and bacteria, similar to neutrophils and monocytes, but they can also produce growth factors such as VEGF to regulate the wound healing process⁶⁵. Therefore, it can be expected that the highest count of macrophages would be in the inflammation phase and proliferation phase. As seen in Figure 5, macrophage counts on week 1 for both groups were the highest compared to week 2 and week 4, showing that in week 1 both groups were still in the inflammation phase. Macrophage count in week 2 of the soy treated group did not change much compared to week 1, but it dropped significantly in week 4. In the control group, macrophage count in week 2 decreased significantly compared to week 1, but it did not have changes in week 4 compared to week 2. In figure 7, vessel count decreased significantly in both groups between week 2 and week 4. However, in Figure 8 and 9 it shows that vessel area and diameter kept decreasing in the soy group but not in the control group. The high count of macrophages in the control group in week 4 may explain why vessel area and diameter did not change or even slightly increase. In figure 16, it showed the correlation of macrophage count and vessel count. The Pearson Correlation Coefficient R is 0.936, suggesting that when macrophage count decreased, vessel count also decreased. VEGF is a potent pro-angiogenic growth factor protein⁶⁶. Macrophages are one of the sources that produce VEGF. One study showed that mutant mice without VEGF solely from cells of myeloid origin had delayed excisional wound healing⁶⁷. The VEGF from macrophages could be the reason that angiogenesis is still active in week 4 of the control group. Figure 10 showed that the wound width decreased from week 1 to week 4 in both wound types and they healed faster between week 1 and week 2. #179 pig model had a similar pattern with the #182 pig model. Figure 11 showed both groups had decreased wound width from week 1 to week 4, but the control group healed faster between week 1 and week 2, week 2 and week 4 while the soy group was faster between week 2 and week 4.

The method for analyzing collagen deposition was to count the total number of normalized data that fell in different intervals. Table 1 and 2 summarized how the count of each interval changed when the wound was healing. In the table, 0-0.3 could be defined as the wound area, 0.3-0.6 was the transitional area, and 0.6-1 was the healthy area. In table 1, the wound area decreased 29.2 % from week 1 to week 4, and the transitional area increased 24.2 % from week 1 to week 4 in the control group. The wound area of the soy group decreased 39 % from week 1 to week 4 and increased 35.5 % in transitional area from week 1 to week 4. These data reflect that in figure 12 and 13, the peak in wound area dropped in the soy group and the peak shifted towards the normal curve more in the soy group than the control group. This showed that collagen deposition increased in the soy group. In Table 2, data representing the #179 pig sample had different results. The wound area of the control group decreased 40.8 % from week 1 to week 4 while the wound area of the soy group decreased 27.5 % from week 1 to week 4. In transitional area, the control group increased 32.8 % from week 1 to week 4 while the soy group increased 25.6 % from week 1 to week 4. Results in Table 2 showed that the control group had better collagen deposition. The difference in results could be due to the method used to analyze collagen deposition. This type of analysis required high quality images. Folds on the tissues and inconsistent staining may have caused errors in data interpretation. The method did prove that as the wound was healing, the peak in the wound area (0-0.3) dropped and shifted towards the normal curve in both pig models.

Macrophage count, vessel area, and vessel diameter all decreased in the soy group, showing that SPS had the ability to improve wound healing. Although collagen deposition did not shift to the healthy area in the soy group of the #182 pig sample compared to normal skin, the decrease in wound area and shift to transitional area showed faster increase of collagen deposition in the soy group compared to the control group. One study indicated when collagen accumulated in the granulation tissue to produce scar, vessels will start to regress and the density of vessels will return to baseline levels⁶⁸. Both groups of the #182 pig sample showed decreased vessel count from week

1 to week 4, but the vessel area and diameter implied that angiogenesis did not finish in the control group.

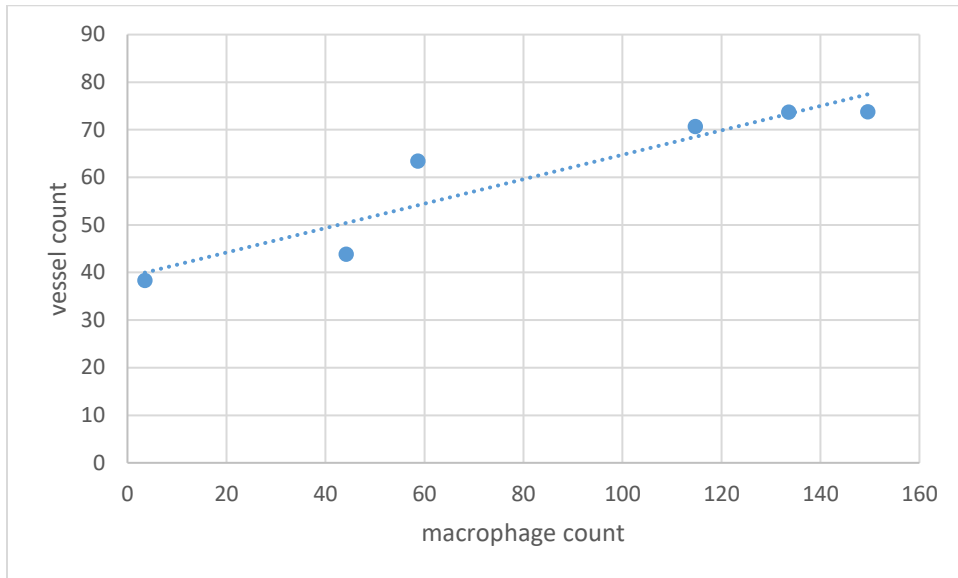


Figure 16. Correlation of vessel count (figure 7) and macrophage count (figure 5) The Pearson Correlation Coefficient $R=0.936$

CHAPTER 6

CONCLUSION AND FUTURE WORK

SPS in this study improved the wound healing process and results showed that soy treated wound in week 4 entered the remodeling phase based on the end of the inflammation phase (decreased macrophages count) and collagen deposition. When macrophage count decreased, vessel count decreased in both wound types but soy treated wound has smaller vessels (smaller vessel area and diameter) compared to control wounds. Certain component in soy protein may help shrink vessels during wound healing process. Control group of #182 may still remain in the inflammation phase in week 4 because macrophage count was higher compared to the soy group. The structure of vessels did not change compared to week 2 and less collagen deposition was observed compared to the soy group. To further confirm how the wound healed, the structure of collagen and vessels could be used. Only matured vessels would be left in the wound and their structure is different from those of newly formed blood vessels²⁸. Collagens form cross-links and align in single and parallel directions in scar tissue, while forming a random basket-weave structure in normal tissue⁶⁹. As shown in figure 5, SPS helped decrease macrophage count significantly in week 4. Future studies can focus on determining what specific components in soy activated or deactivated macrophages. Isoflavones, one of the components in soy, has been proven to have anti-inflammatory effects⁷⁰. Different components can be extracted from soy and cultured with macrophages to further reveal the mechanisms on how SPS may improve the wound healing process.

REFERENCES

1. Metcalfe AD, Ferguson MWJ. Tissue engineering of replacement skin : the crossroads of biomaterials , wound healing , embryonic development , stem cells and regeneration. *J R Soc Soc Interface*. 2007;4(14):413-437. doi:10.1098/rsif.2006.0179.
2. Powell HM, Supp DM, Boyce ST. Influence of electrospun collagen on wound contraction of engineered skin substitutes. *Biomaterials*. 2008;29(7):834-843. doi:10.1016/j.biomaterials.2007.10.036.
3. Enoch S, Shaaban H, Dunn KW. Informed consent should be obtained from patients to use products (skin substitutes) and dressings containing biological material. *J Med Ethics*. 2005;31(1):2-6. doi:10.1136/jme.2003.005272.
4. Reis, R. L., Neves, N. M., Mano, J. F., Gomes, M. E., Marques, A. P., & Azevedo, H. S. (2008). *Natural-based polymers for biomedical applications*. Elsevier.
5. Santin M, Morris C, Standen G, Nicolais L, Ambrosio L. A New Class of Bioactive and Biodegradable Soybean-Based Bone Fillers. *Biomacromolecules*. 2007;8(9):2706-2711. doi:10.1021/bm0703362.
6. Chien KB, Makridakis E, Shah RN. Three Dimensional Printing of Soy Protein Scaffolds for Tissue Regeneration. *Tissue Eng Part C Methods*. 2012;19(6):121026142624002. doi:10.1089/ten.TEC.2012.0383.
7. Lin, L., Perets, A., Har - el, Y. E., Varma, D., Li, M., Lazarovici, P., ... & Lelkes, P. I. (2013). Alimentary ‘green’ proteins as electrospun scaffolds for skin regenerative engineering. *Journal of tissue engineering and regenerative medicine*, 7(12), 994-1008.
8. Meikle, S. T., Standen, G., Salvage, J., De Santis, R., Nicolais, L., Ambrosio, L., & Santin, M. (2012). Synthesis and characterization of soybean-based hydrogels with an intrinsic activity on cell differentiation. *Tissue Engineering Part A*, 18(17-18), 1932-1939.
9. Shimada K, Cheftel JC. Determination of sulfhydryl groups and disulfide bonds in heat-induced gels of soy protein isolate. *J Agric Food Chem*. 1988;36(1):147-153. doi:10.1021/jf00079a038.
10. Brandenburg AH, Weller CL, Testin RF. Edible Films and Coatings from Soy Protein. *J Food Sci*. 1993;58(5):1086-1089. doi:10.1111/j.1365-2621.1993.tb06120.x.
11. Chen L, Remondetto G, Rouabhia M, Subirade M. Kinetics of the breakdown of cross-linked soy protein films for drug delivery. *Biomaterials*. 2008;29(27):3750-3756. doi:10.1016/j.biomaterials.2008.05.025.
12. Chien KB, Shah RN. Novel soy protein scaffolds for tissue regeneration: Material characterization and interaction with human mesenchymal stem cells. *Acta Biomater*. 2012;8(2):694-703. doi:10.1016/j.actbio.2011.09.036.

13. Har-el Y, Gerstenhaber JA, Brodsky R, Huneke RB, Lelkes PI. Electrospun soy protein scaffolds as wound dressings: Enhanced reepithelialization in a porcine model of wound healing. *Wound Med.* 2014;5:9-15. doi:10.1016/j.wndm.2014.04.007.
14. Gosain A, DiPietro LA. Aging and Wound Healing. *World J Surg.* 2004;28(3):321-326. doi:10.1007/s00268-003-7397-6.
15. Mathieu D, Linke J-C, Wattel F. Non-Healing Wounds. In: *Handbook on Hyperbaric Medicine*. Berlin/Heidelberg: Springer-Verlag; 2006:401-428. doi:10.1007/1-4020-4448-8_20.
16. Broughton G, Janis JE, Attinger CE. The Basic Science of Wound Healing. *Plast Reconstr Surg.* 2006;117(SUPPLEMENT):12S-34S. doi:10.1097/01.prs.0000225430.42531.c2.
17. Campos AC, Groth AK, Branco AB. Assessment and nutritional aspects of wound healing. *Curr Opin Clin Nutr Metab Care.* 2008;11(3):281-288. doi:10.1097/MCO.0b013e3282fbd35a.
18. Meszaros, A. J., Reichner, J. S., & Albina, J. E. (2000). Macrophage-induced neutrophil apoptosis. *The Journal of Immunology*, 165(1), 435-441.
19. Mosser, D. M., & Edwards, J. P. (2008). Exploring the full spectrum of macrophage activation. *Nature reviews immunology*, 8(12), 958-969.
20. Gurtner GC, Werner S, Barrandon Y, Longaker MT. Wound repair and regeneration. *Nature.* 2008;453(7193):314-321. doi:10.1038/nature07039.
21. Eming, S. A., Brachvogel, B., Odorisio, T., & Koch, M. (2007). Regulation of angiogenesis: wound healing as a model. *Progress in histochemistry and cytochemistry*, 42(3), 115-170.
22. Szpaderska AM, Walsh CG, Steinberg MJ, DiPietro LA. Distinct Patterns of Angiogenesis in Oral and Skin Wounds. *J Dent Res.* 2005;84(4):309-314. doi:10.1177/154405910508400403.
23. Schultz GS, Davidson JM, Kirsner RS, Bornstein P, Herman IM. Dynamic reciprocity in the wound microenvironment. *Wound Repair Regen.* 2011;19(2):134-148. doi:10.1111/j.1524-475X.2011.00673.x.
24. FUKUMURA D, JAIN RK. Imaging angiogenesis and the microenvironment. *APMIS.* 2008;116(7-8):695-715. doi:10.1111/j.1600-0463.2008.01148.x.
25. Bluff JE, O'Ceallaigh S, O'Kane S, Ferguson MWJ, Ireland G. The microcirculation in acute murine cutaneous incisional wounds shows a spatial and temporal variation in the functionality of vessels. *Wound Repair Regen.* 2006;14(4):434-442. doi:10.1111/j.1743-6109.2006.00142.x.
26. Shaterian A, Borboa A, Sawada R, et al. Real-time analysis of the kinetics of angiogenesis and vascular permeability in an animal model of wound healing. *Burns.* 2009;35(6):811-817. doi:10.1016/j.burns.2008.12.012.

27. Swift ME, Kleinman HK, DiPietro LA. Impaired wound repair and delayed angiogenesis in aged mice. *Lab Invest.* 1999;79(12):1479-1487. <http://www.ncbi.nlm.nih.gov/pubmed/10616199>. Accessed March 19, 2017.
28. Chen RR, Silva EA, Yuen WW, Mooney DJ. Spatio-temporal VEGF and PDGF delivery patterns blood vessel formation and maturation. *Pharm Res.* 2007;24(2):258-264. doi:10.1007/s11095-006-9173-4.
29. Ando J, Yamamoto K. Vascular mechanobiology: endothelial cell responses to fluid shear stress. *Circ J.* 2009;73(11):1983-1992. <http://www.ncbi.nlm.nih.gov/pubmed/19801852>. Accessed March 19, 2017.
30. Xue M, Jackson CJ. COMPREHENSE INVITED REVIEWS Extracellular Matrix Reorganization During Wound Healing and Its Impact on Abnormal Scarring. 2015;4(3):119-136. doi:10.1089/wound.2013.0485.
31. Regan MC, Kirk SJ, Wasserkrug HL, Barbul A. The wound environment as a regulator of fibroblast phenotype. *J Surg Res.* 1991;50(5):442-448. <http://www.ncbi.nlm.nih.gov/pubmed/2038183>.
32. Vedrenne N, Coulomb B, Danigo A, Bonté F, Desmoulière A. The complex dialogue between (myo)fibroblasts and the extracellular matrix during skin repair processes and ageing. *Pathol Biol (Paris).* 2012;60(1):20-27. doi:10.1016/j.patbio.2011.10.002.
33. Klingberg F, Hinz B, White ES. The myofibroblast matrix: implications for tissue repair and fibrosis. *J Pathol.* 2013;229(2):298-309. doi:10.1002/path.4104.
34. Wolfram D, Tzankov A, Püzl P, Piza-Katzer H. Hypertrophic Scars and Keloids—A Review of Their Pathophysiology, Risk Factors, and Therapeutic Management. *Dermatologic Surg.* 2009;35(2):171-181. doi:10.1111/j.1524-4725.2008.34406.x.
35. Hayakawa T, Hashimoto Y, Myokei Y, Aoyama H, Izawa Y. Changes in type of collagen during the development of human post-burn hypertrophic scars. *Clin Chim Acta.* 1979;93(1):119-125. <http://www.ncbi.nlm.nih.gov/pubmed/436291>.
36. Murray, P. J., Allen, J. E., Biswas, S. K., Fisher, E. A., Gilroy, D. W., Goerdts, S., ... & Locati, M. (2014). Macrophage activation and polarization: nomenclature and experimental guidelines. *Immunity*, 41(1), 14-20
37. Gordon S, Taylor PR. Monocyte and macrophage heterogeneity. *Nat Rev Immunol.* 2005;5(12):953-964. doi:10.1038/nri1733.
38. Rees AJ, Stuart LM, Ezekowitz AR, et al. Monocyte and macrophage biology: an overview. *Semin Nephrol.* 2010;30(3):216-233. doi:10.1016/j.semnephrol.2010.03.002.
39. Mosser DM. The many faces of macrophage activation. *J Leukoc Biol.* 2003;73(2):209-212. <http://www.ncbi.nlm.nih.gov/pubmed/12554797>.
40. Brown BN, Ratner BD, Goodman SB, Amar S, Badylak SF. Macrophage

polarization: an opportunity for improved outcomes in biomaterials and regenerative medicine. *Biomaterials*. 2012;33(15):3792-3802. doi:10.1016/j.biomaterials.2012.02.034.

41. Genin M, Clement F, Fattaccioli A, Raes M, Michiels C. M1 and M2 macrophages derived from THP-1 cells differentially modulate the response of cancer cells to etoposide. 2015;1-14. doi:10.1186/s12885-015-1546-9.
42. Mills CD. M1 and M2 Macrophages : Oracles of Health and Disease. 2012;32(6):463-488.
43. Martinez FO, Gordon S. The M1 and M2 paradigm of macrophage activation : time for reassessment. 2014;13(March):1-13. doi:10.12703/P6-13.
44. Janeway CA, Medzhitov R. INNATE IMMUNE RECOGNITION. *Annu Rev Immunol*. 2002;20(1):197-216. doi:10.1146/annurev.immunol.20.083001.084359.
45. Song E, Ouyang N, Hörbelt M, Antus B, Wang M, Exton MS. Influence of Alternatively and Classically Activated Macrophages on Fibrogenic Activities of Human Fibroblasts. *Cell Immunol*. 2000;204(1):19-28. doi:10.1006/cimm.2000.1687.
46. Schnoor M, Cullen P, Lorkowski J, et al. Production of type VI collagen by human macrophages: a new dimension in macrophage functional heterogeneity. *J Immunol*. 2008;180(8):5707-5719. <http://www.ncbi.nlm.nih.gov/pubmed/18390756>.
47. Gratchev A, Guillot P, Hakiy N, et al. Alternatively activated macrophages differentially express fibronectin and its splice variants and the extracellular matrix protein betaIG-H3. *Scand J Immunol*. 2001;53(4):386-392. <http://www.ncbi.nlm.nih.gov/pubmed/11285119>.
48. D'Andrea, A., Ma, X., Aste-Amezaga, M., Paganin, C., & Trinchieri, G. (1995). Stimulatory and inhibitory effects of interleukin (IL)-4 and IL-13 on the production of cytokines by human peripheral blood mononuclear cells: priming for IL-12 and tumor necrosis factor alpha production. *Journal of Experimental Medicine*, 181(2), 537-546..
49. Young VR. Soy protein in relation to human protein and amino acid nutrition. *J Am Diet Assoc*. 1991;91(7):828-835. <http://www.ncbi.nlm.nih.gov/pubmed/2071798>.
50. Wang, H. J., & Murphy, P. A. (1996). Mass balance study of isoflavones during soybean processing. *Journal of Agricultural and Food Chemistry*, 44(8), 2377-2383.
51. Verdrengh M, Jonsson IM, Holmdahl R, Tarkowski A. Genistein as an anti-inflammatory agent. *Inflamm Res*. 2003;52(8):341-346. doi:10.1007/s00011-003-1182-8.
52. Frykberg RG, Banks J. Challenges in the Treatment of Chronic Wounds. *Adv Wound Care*. 2015;4(9):560-582. doi:10.1089/wound.2015.0635.

53. Jackson WM, Nesti LJ, Tuan RS. Concise review: clinical translation of wound healing therapies based on mesenchymal stem cells. *Stem Cells Transl Med.* 2012;1(1):44-50. doi:10.5966/sctm.2011-0024.
54. Greenhalgh DG. The role of apoptosis in wound healing. *Int J Biochem Cell Biol.* 1998;30(9):1019-1030. doi:10.1016/S1357-2725(98)00058-2.
55. Stashak TS, Farstvedt E, Othic A. Update on wound dressings: Indications and best use. *Clin Tech Equine Pract.* 2004;3(2):148-163. doi:10.1053/j.ctep.2004.08.006.
56. Santulli, G. (Ed.). (2013). Angiogenesis: insights from a systematic overview
57. Ding Y-H, Luan X-D, Li J, et al. Exercise-Induced Overexpression of Angiogenic Factors and Reduction of Ischemia / Reperfusion Injury in Stroke. *Curr Neurovasc Res.* 2004;1(5):411-420. doi:10.2174/1567202043361875.
58. Ruszczak Z. Effect of collagen matrices on dermal wound healing. *Adv Drug Deliv Rev.* 2003;55(12):1595-1611. doi:10.1016/j.addr.2003.08.003.
59. Wolfram D, Tzankov A, Püzl P, Piza-Katzer H. Hypertrophic Scars and Keloids—A Review of Their Pathophysiology, Risk Factors, and Therapeutic Management. *Dermatologic Surg.* 2009;35(2):171-181. doi:10.1111/j.1524-4725.2008.34406.x.
60. Eming SA, Krieg T, Davidson JM. Gene therapy and wound healing. *Clin Dermatol.* 2007;25(1):79-92. doi:10.1016/j.clindermatol.2006.09.011.
61. Werner S, Grose R. Regulation of Wound Healing by Growth Factors and Cytokines. *Physiol Rev.* 2003;83(3). <http://physrev.physiology.org/content/83/3/835.short>.
62. Barrientos S, Stojadinovic O, Golinko MS, Brem H, Tomic-Canic M. Growth factors and cytokines in wound healing. *Wound Repair Regen.* 2008;16(5):585-601. doi:10.1111/j.1524-475X.2008.00410.x.
63. Clark RAF, ed. *The Molecular and Cellular Biology of Wound Repair.* Boston, MA: Springer US; 1988. doi:10.1007/978-1-4899-0185-9.
64. Epstein FH, Singer AJ, Clark RAF. Cutaneous Wound Healing. *N Engl J Med.* 1999;341(10):738-746. doi:10.1056/NEJM199909023411006.
65. Manuscript A. Inflammation and wound healing : The role of the macrophage. 2013;16(2008):19-25. doi:10.1017/S1462399411001943.Inflammation.
66. Nissen NN, Polverini PJ, Koch AE, Volin M V, Gamelli RL, DiPietro LA. Vascular endothelial growth factor mediates angiogenic activity during the proliferative phase of wound healing. *Am J Pathol.* 1998;152(6):1445-1452. <http://www.ncbi.nlm.nih.gov/pubmed/9626049>.
67. Stockmann C, Kirmse S, Helfrich I, et al. A wound size-dependent effect of myeloid cell-derived vascular endothelial growth factor on wound healing. *J Invest*

Dermatol. 2011;131(3):797-801. doi:10.1038/jid.2010.345.

68. Tonnesen MG, Feng X, Clark RA. Angiogenesis in wound healing. *J Invest Dermatol Symp Proc.* 2000;5(1):40-46. doi:10.1046/j.1087-0024.2000.00014.x.
69. Ehrlich HP, Krummel TM. Regulation of wound healing from a connective tissue perspective. *Wound Repair Regen.* 1996;4(2):203-210. doi:10.1046/j.1524-475X.1996.40206.x.
70. Chacko BK, Chandler RT, Mundhekar A, et al. Revealing anti-inflammatory mechanisms of soy isoflavones by flow: modulation of leukocyte-endothelial cell interactions. *AJP Hear Circ Physiol.* 2005;289(2):H908-H915. doi:10.1152/ajpheart.00781.2004.